American Mineralogist, Volume 62, pages 646–665, 1977

Titanium-containing silicate garnets. II. The crystal chemistry of melanites and schorlomites

FRANK E. HUGGINS, DAVID VIRGO AND H. GERHARD HUCKENHOLZ[1]

Geophysical Laboratory, Carnegie Institution of Washington
Washington, D. C. 20008

Abstract

A suite of eleven melanite and schorlomite garnets, mostly from alkaline igneous rocks, has been studied by means of the electron microprobe and Mössbauer spectroscopy. The TiO_2 contents of these garnets ranged from 2.5 to 16.5 weight percent. The Mössbauer spectra showed the presence of up to five distinct kinds of iron absorption doublets within the garnet structure: ferric iron in octahedral and tetrahedral coordination, and ferrous iron in dodecahedral, octahedral, and tetrahedral coordination. Fe^{2+} in octahedral or tetrahedral coordination, rather than Ti, is responsible for the deep red-black color and correlated features in the optical absorption spectrum of these garnets. The Mössbauer parameters of the absorption due to tetrahedral ferrous iron are unusually small and are consistent with electron-hopping phenomena. The coexistence of ferrous and ferric iron on both the octahedral and the tetrahedral sites is unusual for the garnet structure, and is believed to be suggestive of low oxygen fugacities at the time of formation of the garnets. The $Fe^{3+}/\Sigma Fe$ as determined by Mössbauer spectroscopy varied from 0.00 to 0.26 and agreed generally with the total number of reducing cations as determined by wet chemistry or by calculation from the electron microprobe analysis, but in some of the samples, small amounts of other reducing species, presumably Ti^{3+}, were also required to account for significant differences between the methods. Estimates of $Ti^{3+}/\Sigma Ti$ for these garnets exceeded 0.10 in only one sample, for which the ratio was as high as 0.25.

No one coupled-substitution mechanism can account for all the Ti in the garnet structure, and two or more of the following substitutions have to be invoked to account for the Ti substituted into the garnet:

$$Ti^{4+} \rightleftarrows Si^{4+} \text{ or } M^{2+} + Ti^{4+} \rightleftarrows 2M^{3+} \text{ or } Ti^{3+} \rightleftarrows M^{3+}.$$

The distribution of iron between the octahedral sites and those tetrahedral sites not occupied by Si is compatible with the scheme established for Fe^{3+} in synthetic garnets only if the oxidation states of the iron cations are disregarded. This implies that, at high temperatures, extensive electron-hopping between Fe cations and presumably Ti cations occurs rapidly so that no distinction of different valence states of the Fe and Ti cations can be made with respect to cation exchange.

Introduction

Published investigations have shown that the crystal chemistry of naturally occurring, Ti-rich silicate garnets is quite complex. Such investigations have attempted primarily to establish the oxidation states of Fe and Ti and the location of Al, Fe, and Ti cations within the garnet structure, but have not been entirely successful because the techniques used were not sufficient to overcome the complexities (Dowty, 1971; Huggins *et al.*, 1977).

Mössbauer spectroscopy is specific for elucidating details of the crystal chemistry of Fe cations and therefore provides a convenient base for interpreting the crystal chemistry of the elements in the garnet structure. In the present study, Mössbauer spectra of melanites and schorlomites were used in conjunction with electron microprobe analyses and data on synthetic Ti-rich garnets (Huggins *et al.*, 1977) to obtain or infer crystallochemical information concerning all the major elements in titanium garnets.

Silicate garnets lacking Ti usually have a very regular crystal chemistry, which can be represented by the general formula (after Novak and Gibbs, 1971)

$$\{M^{2+}\}_3[M^{3+}]_2Si_3O_{12}.$$

It is inferred from this formula that divalent cations

---

[1] Permanent address: Mineralogisch-Petrographisches Institut der Universität, Munich, Germany.

are found in the eight-coordinated site, trivalent cations are found in the octahedral site and quadrivalent cations. *i.e.*, Si^{4+}, are found in the tetrahedral sites, exclusively. Almost all chemical analyses of Ti-free garnets do indeed indicate a 3:2:3 ratio for $M^{2+}:M^{3+}:Si^{4+}$.

On the other hand, chemical analyses of natural Ti-rich garnets deviate from the above general formula, usually in one or more of the following ways (Zedlitz, 1933; Dowty, 1971; Huckenholz, 1969): The number of divalent cations exceeds 3.0; the number of trivalent cations is less than 2.0; the number of quadrivalent cations (Si + Ti) exceeds 2.0. Owing to these deviations, it may be concluded that the substitution of Ti into the garnet structure comes about not only at the expense of Si but at the expense of other elements as well. Huckenholz (1969) advocated the following coupled substitution at the octahedral site:

$$2M^{3+}\mathrm{VI} \rightleftharpoons M^{2+}\mathrm{VI} + \mathrm{Ti}^{4+}\mathrm{VI}$$

This substitution is, of course, indicated by the deviations of the composition of Ti-rich garnets from the ideal garnet stoichiometry. Much earlier, however, Zedlitz (1933) suggested that if the reduced cations that are oxidized in the course of a wet-chemical analysis are Ti^{3+} rather than Fe^{2+}, the deviation from the ideal garnet formula is minimized. Subsequently, earth scientists have been undecided on whether to treat the reduced cations in melanite and schorlomite analyses as all Fe^{2+}, all Ti^{3+}, or some combination, until studies could be made that characterize the oxidation states of the two elements. Investigations using optical absorption spectroscopy have been conducted for this purpose (Manning and Harris, 1970; Moore and White, 1971; Dowty, 1971; Burns, 1972), but interpretation of the spectra is ambiguous, and the technique is not sufficiently quantitative to provide accurate values for Fe^{2+}/Fe^{3+} or Ti^{3+}/Ti^{4+}.

Calibrated Mössbauer studies provide accurate estimates of Fe^{2+}/Fe^{3+}, and hence, by subtracting the amount of Fe^{2+} from the total reducing capacity (that is, the number of reduced cations oxidized in the course of a wet-chemical analysis), the amount of Ti^{3+} can be estimated. No difference between the Mössbauer and wet-chemical determinations for one schorlomite led Dowty (1971) to suggest that the amount of Ti^{3+} was negligible; however, significant differences from other garnets were found by Burns and Burns (1971), Burns (1972), and Whipple (1973), indicating that Fe^{2+} did not account for all the reducing capacity of natural Ti-containing garnets. In this study, a similar comparison for eleven melanites and schorlomites is made between Mössbauer determinations and determinations based on chemical methods, principally electron microprobe analyses calculated according to the garnet stoichiometry, to determine the oxidation states of the Fe and Ti cations. In addition, by using the site preference data established for Al, Fe^{3+}, and Ti^{4+} cations in synthetic Ti-containing garnets (Huggins *et al.*, 1977), the location of the cations in these natural garnets is investigated.

Determination of the location and oxidation states of cations in the garnet structure is useful not only for establishing crystal-chemical principles, but also for providing data of importance to the petrology of the host rocks. It is well known that the distribution of two or more cations between nonequivalent sites in a mineral structure can be related to the thermal history of the mineral. In a similar fashion, the coexistence of cations of different oxidation states at similar crystallographic positions may reflect the conditions of oxygen fugacity under which the mineral crystallized.

Experimental techniques

Electron microprobe analyses

Chemical analyses were performed using a MAC electron microprobe operating at 15 kV. Automatic operating procedures and data-reduction techniques based on the Bence-Albee matrix corrections and standards of known composition were used. These techniques are similar to those described by Finger and Hadidiacos (1972). Seven elements (Ca, Mn, Mg, Fe, Ti, Al, Si) were measured in this manner and were assumed to approximate the total chemical composition of the garnet. An additional fourteen elements were analyzed on a qualitative basis (*i.e.*, no matrix corrections), so that elements would not be overlooked that might possibly be present in significant quantities (see, for example, the minor-element concentrations reported by Erickson and Blade (1963) for schorlomites from Magnet Cove, Arkansas).

Mössbauer spectroscopy

Mössbauer data were obtained and fitted in a manner similar to that described previously (Huggins *et al.*, 1977). The presence of Fe^{2+} in the garnets, however, necessitated fitting the data with up to six unconstrained Lorentzian peaks. In order to reduce the differences between the ferrous and ferric recoil-free fractions, which are known to be significantly different for garnets at room temperature (Whipple, 1973; Amthauer *et al.*, 1976), and to improve the resolution of the ferrous peaks, experiments were carried out with the samples cooled to 77K by using an evacuated, liquid-nitrogen cooled Dewar system.

Description of samples

Sixteen melanite and schorlomite garnets were investigated in the course of this study. Macroscopically, all garnets were either very deep brown or black, and their morphology varied from euhedral to anhedral. Broken surfaces generally were highly reflective; some of the garnets had a metallic luster. In powder form, the colors varied from pale yellow-brown to dark gray with a purple tint; in grain mounts, the color varied from orange-brown to almost opaque with a deep smoky-purple at the edges.

All except two of the samples came from alkaline igneous rocks, of which about half were associated with carbonatite complexes. The two exceptions were from a skarn (sample DW) and from a serpentinized peridotite body (sample SB). In Table 1 the samples are described in more detail.

The garnets were separated from the host rocks, when necessary, by magnetic or heavy-liquid techniques, or both; final hand-picking of the crushed garnets under a binocular microscope ensured a high degree of purity for all samples.

Results

Electron microprobe experiments

Qualitative analyses (Table 2) established that Na, V, and Zr were the only elements likely to be present in measurable amounts, except for the seven major elements. The amounts of these minor elements were less than 0.3 weight percent, however, and hence more quantitative analyses for these elements were not performed. Quantitative analyses for all seven major oxides are listed in Table 3 for samples that were also subjected to Mössbauer experimentation. Electron microprobe results for other garnets, mostly strongly zoned samples that were not useful for Mössbauer experimentation, are listed in Table A 1 of the Appendix.

The oxide weight-percentage data were first reduced on a formula basis assuming eight cations per formula unit. The cation-to-anion ratios were then adjusted to 8:12, the regular garnet stoichiometry, by "reduction" of some of the ferric iron to ferrous. This adjustment could, of course, also be achieved by reduction of TiO_2 to Ti_2O_3, as this element may possibly exhibit variable valency in the garnets. Nevertheless, in this way the total number of reduced cations, assuming a stoichiometric formula, can be estimated. The formulae of the garnets, with all the calculated reduced cations as Fe^{2+}, are shown in Table 3. Although such calculations of Fe^{2+} accumulate all the errors associated with the electron microprobe analysis, making the values somewhat imprecise (Finger, 1972), a more serious systematic error may arise from possible omission of minor elements, particularly sodium. By omitting quadrivalent elements, such as Zr, the calculation of the actual amount of Fe^{2+} is an underestimate, whereas by omitting monovalent or divalent cations, the calculation is an overestimate. For instance, the addition of about 0.30 weight percent Na_2O to sample OL, as indicated by qualitative analysis (Table 2), causes the calculated $Fe^{2+}/\Sigma Fe$ to be lowered from 0.17 without Na to 0.11. Hence, each 0.1 weight percent Na_2O ignored would reduce the $Fe^{2+}/\Sigma Fe$ by about 0.02; the effect of other elements, however, is much smaller. Of the samples investigated here, the effect of sodium would appear to be significant for sample OL, but within the precision of the calculation for all other samples.

Of the eleven analyses in Table 2, two (SB and DW) apparently do not fit the usual garnet formula because calcium exceeds 3.0 cations per formula unit. The reason for this discrepancy is not obvious. The presence of significant amounts of other elements is unlikely, given the oxide totals and the qualitative search for other elements (Table 2); the only exception might be H_2O, present in the form of a hydrogarnet component. Infrared spectra of these garnets, dried overnight at 180°C, however, did not show any peaks at $\sim$3400–3600 cm^{-1} that might be attributed to a hydrogarnet component.

In all samples except Ar, the sum Ca+Mn+Mg exceeds 3.0 cations per formula unit, implying that some divalent cations must be on octahedral sites or that some of the Mn in these analyses may in fact be octahedral Mn^{3+} or some combination. Also, in all samples, the sum Si+Ti exceeds 3.0 cations per formula unit, demonstrating that some Ti must be on octahedral sites. As concluded in most previous studies, on the basis of just the chemical evidence, it appears necessary that the coupled substitution

$$M^{2+} + Ti^{4+} \rightleftharpoons 2M^{3+} \; (M^{2+} = Mg^{2+} \text{ or possibly } Mn^{2+} \text{ or } Ca^{2+})$$

is operative at the octahedral sites in the garnet structure. The question of whether a similar substitution occurs with Fe^{2+} is answered in the next section, using evidence from Mössbauer spectroscopy.

Table 1. Description of samples

Symbol*	Description
	Unzoned Samples
O (2.48)†	Ijolite from Oka carbonatite complex, Quebec. Anhedral crystals. Variable orange-brown color in thin section. Garnets contained calcite and zeolite (?) inclusions. Rock supplied by M. Rosenhauer.
F (2.53)	Calc-silicate bomb in pyroclastics from the Alban Hills, Frascati, Italy. Euhedral crystals (up to 20 mm). Brown in grain mount. Collected by H. G. Huckenholz.
LB (3.56)	Nepheline syenite from Loch Borolan, Scotland. Same sample as No. 4, Howie and Woolley (1968). Coarse grains supplied by R. A. Howie.
OL (8.57)	Volcanic ash from Oldoinyo Lengai, Tanzania. Small euhedral crystals. Deep bluish red in grain mount. Magnetic separate of ash supplied by Th. G. Sahama.
DW (10.84)	From a monomineralic vein in a massive skarn deposit within the Precambrian basement complex, northern Red Sea Hills, Sudan. Brown in grain mount. Same locality as No. 9, Howie and Woolley (1968). Coarse powder supplied by R. A. Howie.
K (12.37)	Phonolite dike from Oberrotweil, Kaiserstuhl, West Germany. Euhedral crystals (3-5 mm). Deep purple in grain mount. Collected by H. G. Huckenholz.
Iv (12.72)	Pegmatoid in ijolite from Iivaara alkaline igneous complex, Finland. Brown-orange in grain mount. Massive single crystal supplied by Th. G. Sahama.
ML (13.18)	Melteigite from Iivaara alkaline igneous complex, Finland. Anhedral crystals. Deep brown in grain mount. Same specimen (ML 9/54) as described by Lehijärvi (1960). Rock supplied by Th. G. Sahama.
4562 (13.75)	Nepheline pegmatite dike in pyroxenite, from Afrikanda, Kola, USSR. Anhedral crystals. Rock supplied by Th. G. Sahama.
R (14.34)	Agglomerate from Rusinga Island, Uganda. Euhedral single crystal (~10 mm). Deep purple in grain mount. USNM 107272, supplied by J. S. White, Jr.
Ar (16.46)	Schorlomite-wollastonite-titanaugite vein in pegmatitic pyroxenite from Ardnamurchan, Scotland. Deep purple in grain mount. Similar to sample No. 10, Howie and Woolley (1968). Rock section supplied by S. O. Agrell.
	Zoned Samples
SB	In a chlorite matrix within blocks of serpentinized peridotite near the Dallas Gem Mine, San Benito County, California. Euhedral crystals (2-10 mm). In grain mount crystals have pale yellow rim that abruptly grades into opaque except for deep red-blue tinge at broken edge of grain. USNM R15546-5, supplied by J. S. White, Jr.
AD	Ijolite from Amba Dongar carbonatite complex, India. Same sample as No. 6, Howie and Woolley (1968). Coarse grains supplied by R. A. Howie.
4718	Schorlomite in calcite from carbonatite complex, Habazero, Kola, USSR. Rock supplied by Th. G. Sahama.
KO	From carbonatite complex, Kurovni, Kola, USSR. USNM 103154, supplied by H. G. Huckenholz.
MC	Ijolite from carbonatite complex, Magnet Cove, Arkansas. USNM 97012, supplied by H. G. Huckenholz.

*Unzoned samples listed in order of increasing titanium content.
†Numbers in parentheses are wt % TiO_2 in garnet.

Mössbauer data and interpretation

Mössbauer spectra of some of the samples, representing the range of chemical variation of the garnets, are shown in Figures 1–5. The spectra were fitted without constraints, using as many peaks as were apparent visually; if more complicated fits are attempted, convergence is not achieved unless constraints are applied to certain peak parameters. By using the unconstrained fitting procedure, the spectra were fitted with up to six peaks, although usually one or more of the peaks either were absent or could not be adequately resolved. Except for spectra in which minor peaks were not adequately resolved, the distri-

Table 2. Minor element data for melanites and schorlomites*

	O	F	LB	SB	OL	DW	K	Iv	ML	R	Ar
Na	-	+	+	-	0.3	-	0.1	0.1	0.1	+	0.1
Zr	-	-	0.1	-	0.1	+	0.1	-	-	0.1	-
V	0.2	0.2	0.1	-	0.1	+	0.2	-	-	0.1	-
K	-	-	-	-	-	-	-	-	-	-	-
Cr	-	-	-	-	-	0.1	+	-	-	-	+
Sc	-	-	-	-	-	+	-	-	-	+	-
Ni	+	-	-	-	+	+	+	-	-	-	+
Ce	+	+	+	-	-	-	-	-	-	-	-

*Minus sign indicates that element was not detected; plus sign, element detected, but less than 0.1%. Numerical values are no more accurate than ±50%. Other elements sought but not found in any sample were P, S, Cl, Co, Cu, Zn, Ba.

bution of ferrous and ferric iron between the different sites could be determined using the fitting scheme described above. Data on peak positions, areas, and widths are listed in Table 4.

The assignment of the spectral peaks to specific Fe cations and coordination numbers was based on the spectrum of sample Ar (Fig. 5), which is the only one requiring a fit with six peaks. The three peaks at low velocity (A_{IV}, A_{VI}, and A_c) are similar in position to the peaks in the synthetic ferric garnets (Huggins *et al.*, 1977), and correspond, respectively, to the low-velocity tetrahedral and octahedral peaks and the composite high-velocity peak of the ferric absorption. The three peaks B_{IV}, B_{VI}, and B_{VIII} are at velocities too high for ferric iron and must therefore involve ferrous iron. They are also all at velocities too high to be possibly paired with each other: any such pairing results in an isomer shift that is much too high for ferrous iron. The only acceptable interpretation is that these peaks are high-velocity components of three distinct ferrous doublets, the low-velocity components of which are hidden under the ferric absorption. In keeping with general trends concerning the isomer shift (IS) and quadrupole splitting (QS) values of Fe^{2+} as a function of coordination (see, for example, Burns *et al.*, 1972), these peaks are assigned to tetrahedral, octahedral and dodecahedral ferrous iron with increasing velocity. The low-velocity peaks of these ferrous doublets are assumed to be primarily located underneath peak A_{IV} at 77 K. The evidence for this assumption is as follows: first, on the basis of known IS and QS data for ferrous iron in 4, 6, and 8 coordination in silicates and the measured position of the high-velocity peaks, the position of peak A_{IV} corresponds quite closely to the anticipated positions of the low-velocity components of the ferrous doublets. Secondly, the difference in position of peak B_{IV} be-

Table 3. Chemical analyses and formulae of garnets

	O	F	LB	SB*	OL	DW	K	Iv	ML	R	Ar
						Analyses, wt %					
SiO_2	34.77	35.49	34.57	33.44	30.89	27.14	28.70	28.38	28.95	28.17	26.15
TiO_2	2.48	2.53	3.56	8.57	10.84	12.37	12.72	13.18	13.20	14.34	16.46
Al_2O_3	4.68	6.57	2.69	1.55	0.70	5.23	2.24	0.93	1.02	1.05	3.51
Fe_2O_3†	23.17	20.62	25.43	20.58	24.36	20.44	22.19	23.42	22.84	22.04	21.15
MgO	0.45	0.57	0.40	0.71	0.47	0.86	0.89	0.85	0.96	0.89	0.52
MnO	0.99	0.28	0.64	0.13	0.40	0.09	0.41	0.20	0.25	0.33	0.38
CaO	32.58	33.01	33.36	33.66	32.64	30.66	31.43	31.54	31.77	31.65	31.18
Totals	99.12	99.07	100.65	98.64	100.30	99.79	98.58	98.50	98.12	98.47	99.35
						Formulae, assuming 8:12 cation-to-anion ratio					
Si	2.900	2.924	2.868	2.834	2.623	2.276	2.470	2.472	2.492	2.442	2.250
Ti	0.154	0.157	0.222	0.546	0.692	0.780	0.823	0.863	0.854	0.935	1.065
Al	0.458	0.638	0.263	0.155	0.070	0.517	0.227	0.101	0.103	0.107	0.353
Fe^{3+}	1.433	1.201	1.557	1.083	1.299	1.290	1.186	1.228	1.204	1.140	1.017
"Fe^{2+}"‡	0.020	0.077	0.030	0.229	0.257	0.000	0.251	0.268	0.275	0.298	0.351
Mg	0.054	0.070	0.049	0.090	0.059	0.107	0.114	0.120	0.123	0.115	0.065
Mn	0.069	0.020	0.045	0.009	0.029	0.006	0.030	0.016	0.018	0.024	0.025
Ca	2.912	2.914	2.965	3.055	2.970	3.024	2.898	2.932	2.930	2.939	2.874
ΣFe	1.453	1.278	1.587	1.312	1.566	1.290	1.437	1.496	1.479	1.438	1.368
"Fe^{2+}"/ΣFe	0.015	0.06	0.02	0.17	0.17	0.00§	0.17	0.18	0.19	0.21	0.26

*SB is an average of all zones--see Table A1 of the Appendix for details on chemical differences of zones.
†All iron as Fe_2O_3.
‡Total number of reduced cations, not just Fe^{2+} (see text).
§Σ oxygen = 11.96.

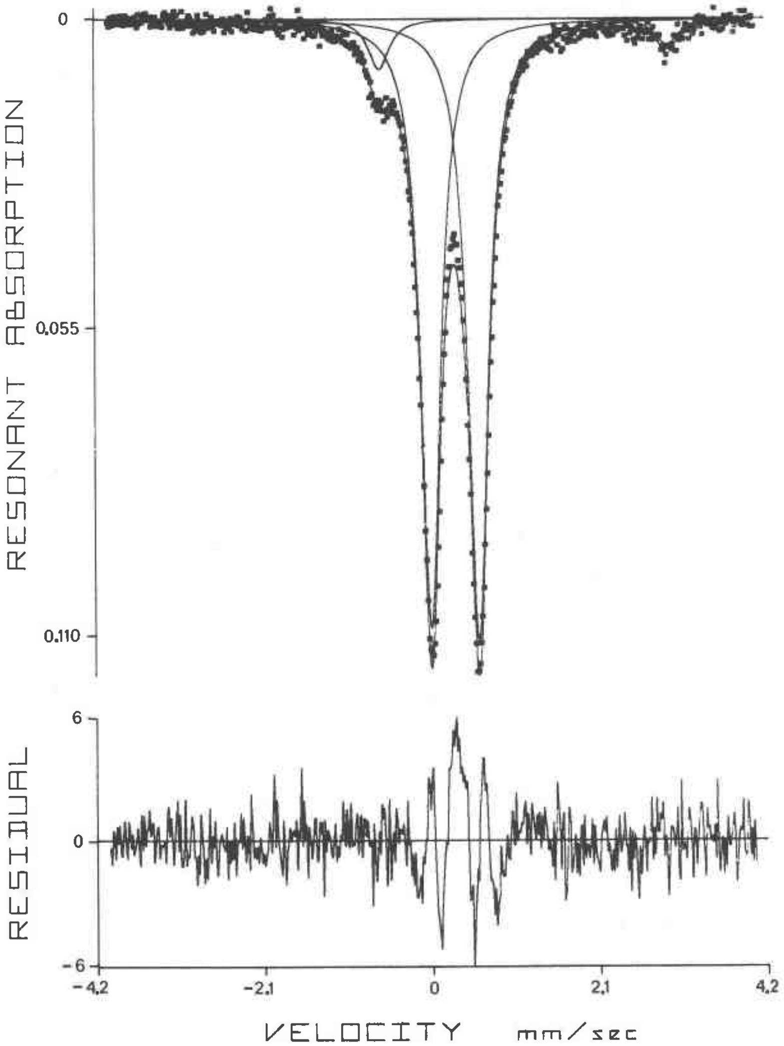

Fig. 1. Mössbauer spectrum of melanite from Frascati, Italy; sample F. Spectrum is fitted to four peaks.

tween 298 and 77 K (Fig. 6, Table 4) indicates that this peak shifts very rapidly to high velocity with decreasing temperature, reflecting a very temperature-sensitive quadrupole splitting. Another obvious difference between the two spectra is the enhancement in area of peak A_{IV} at 77 K relative to that at 298 K, as a result of the low-velocity component of B_{IV} moving under A_{IV}. Hence, in Table 5 the isomer shift and quadrupole splitting values for the ferrous absorptions are calculated on the assumption that the position of A_{IV} corresponds to the position of the low-velocity peaks of the ferrous doublets, as indicated in Figure 5.

In theory, these garnet spectra should be fitted with two peaks for each different kind of Fe cation in the mineral, implying that the spectra should be fitted with up to ten peaks, reflecting up to five different kinds of Fe cation. By representing the low-velocity region of the spectrum simply by two peaks, A_{IV} and A_{VI}, rather than up to five peaks, deviations of the calculated envelope from the observed data in this region of the spectrum can be seen from the residuals in Figures 1–4. Adding more peaks to the fit with or without constraints on some of the parameters does not result in a better fit, because their variable parameters are influenced by another source of discrepancy between calculated fit and observed data, namely peak broadening due to next-nearest neighbor interactions about the ferric iron, which is apparent even when no Fe^{2+} is present (*e.g.*, Fig. 3). For this reason, constrained fits with additional peaks are probably no more correct or informative than the uncon-

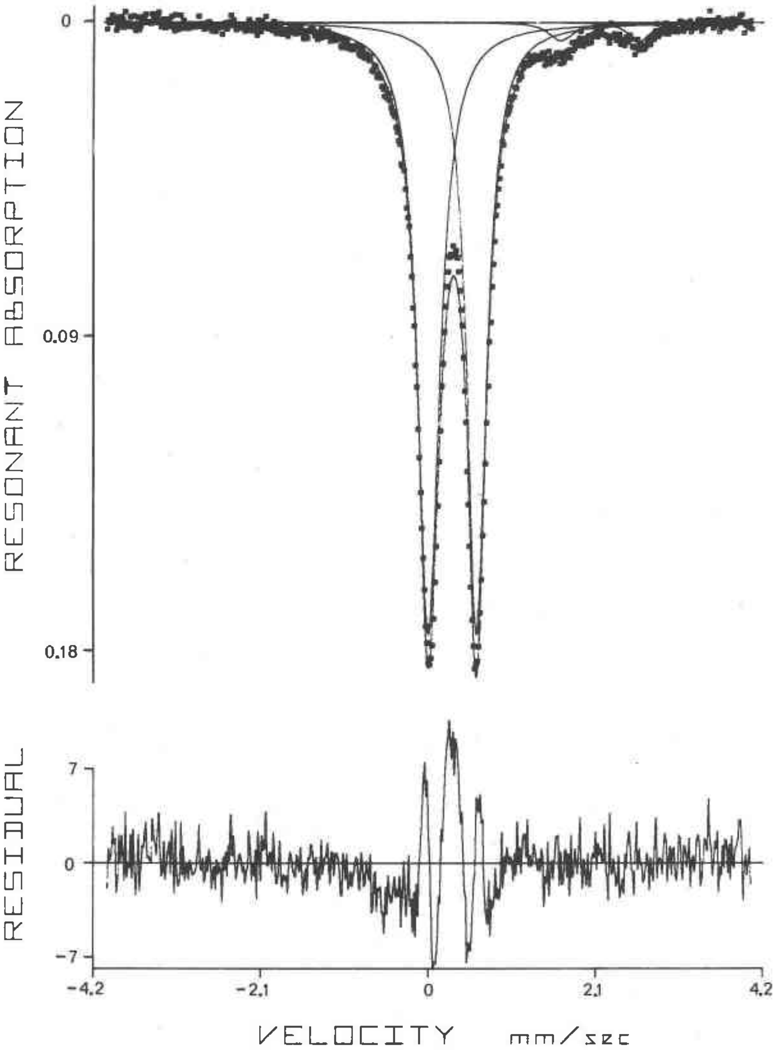

Fig. 2. Mössbauer spectrum of melanite from Dallas Gem Mine, San Benito County, California; sample SB. Spectrum is fitted to four peaks.

strained fits used here. As a result of adopting the unconstrained fitting procedure, the values of isomer shift and quadrupole splitting shown in Table 5 may be subject to small but significant systematic errors; however, the choice of fitting procedure is not expected to affect significantly the ratios for the different kinds of Fe cations in the garnets (Table 4). It is these ratios, of course, that are of prime interest in this study.

Although sample Ar is the only one that provides convincing evidence for both octahedral and dodecahedral ferrous iron in the same sample, a number of other samples was found to have the peak at highest velocity at a position intermediate to octahedral ferrous and dodecahedral ferrous positions. As indicated in Tables 4 and 5, this peak most probably represents a composite Fe^{2+}VI and Fe^{2+}VIII absorption. As a result of the weak absorption of these peaks (<1%), the data for such peaks are statistically of low quality, so that fitting them to more than one Lorentzian peak is usually not warranted.

The presence of small peaks in the Mössbauer spectrum resulting from ferrous iron in octahedral coordination in the garnet indicates that the following coupled substitution, similar to that suggested for other M^{2+} cations, is operative at the octahedral sites in the garnet: $Fe^{2+} + Ti^{4+} \rightleftharpoons 2M^{3+}$. Other possible substitutions that have been suggested for melanites and schorlomites, such as Fe^{3+}VI $\rightleftharpoons$ Ti^{3+}VI (Manning and Harris, 1970; Burns, 1972) and $2Ti^{4+}$VI +

$Fe^{2+}IV \rightleftharpoons 2M^{3+}VI + Si^{4+}IV$ (Dowty, 1971), are discussed in the next section.

Discussion

Comparison of ferrous-ferric ratios and the presence of Ti^{3+}

In this study, the ferrous-ferric ratio can be estimated in two ways, by Mössbauer spectroscopy and from chemical analyses. A comparison of the values for garnets analyzed by chemical and Mössbauer methods is made in Table 6. As may be inferred from this table and Figure 7, most of the reduced cations do indeed appear to be Fe^{2+}. However, there is a definite bias in the data to one side of the 1:1 line in Figure 7, which indicates the presence of other reduced cations. This bias is particularly evident when the Mössbauer Fe^{2+} content is low. Even allowing for possible differences in recoil-free fractions (that might increase $Fe^{2+}/\Sigma Fe$, as measured by Mössbauer spectroscopy, by up to 10 percent of the value), and the effect of Na and other trace elements (negligible except possibly for sample OL), it appears likely that samples SB, GN4, and GN3, and possibly Iv have small but significant amounts of another reducing cation present, most probably Ti^{3+}. Hence, it appears possible that in titanium garnets the substitution $Ti^{3+} \rightleftharpoons M^{3+}$ may occur, but in most of the specimens studied it amounts to no more than 5 percent of the total trivalent cations. For sample SB, on the basis of microprobe data, this substitution may be somewhat higher, about 8 percent. This finding agrees in prin-

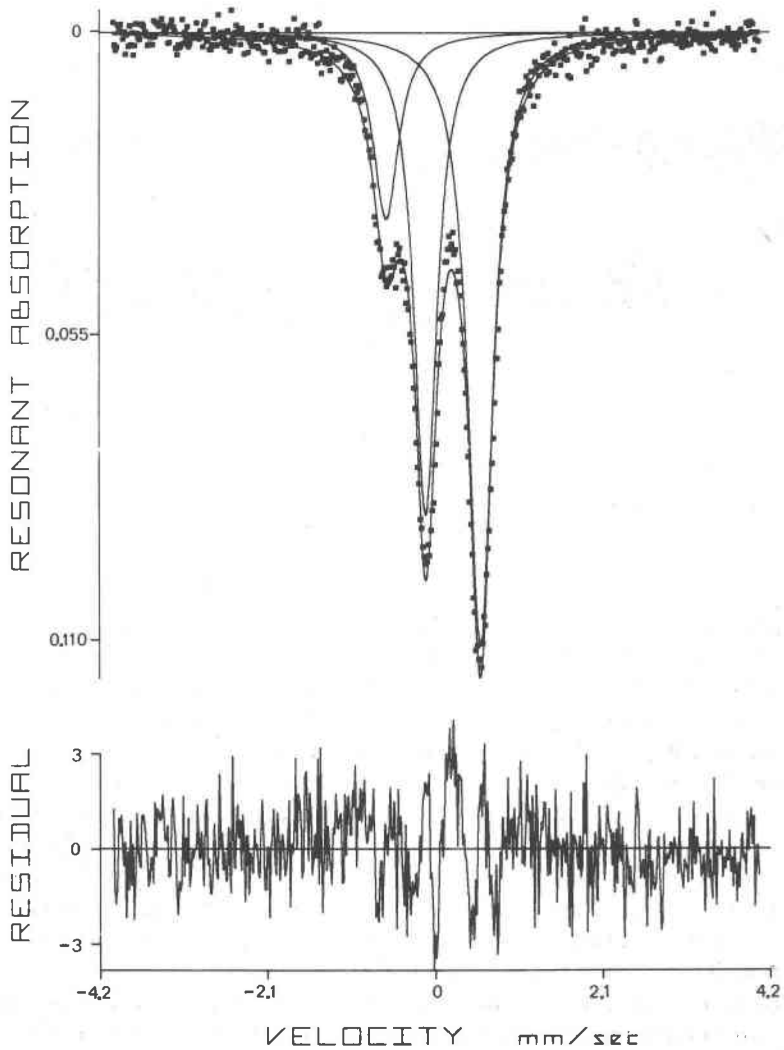

Fig. 3. Mössbauer spectrum of schorlomite from Dirbat Well, Sudan; sample DW. Spectrum is fitted to three peaks.

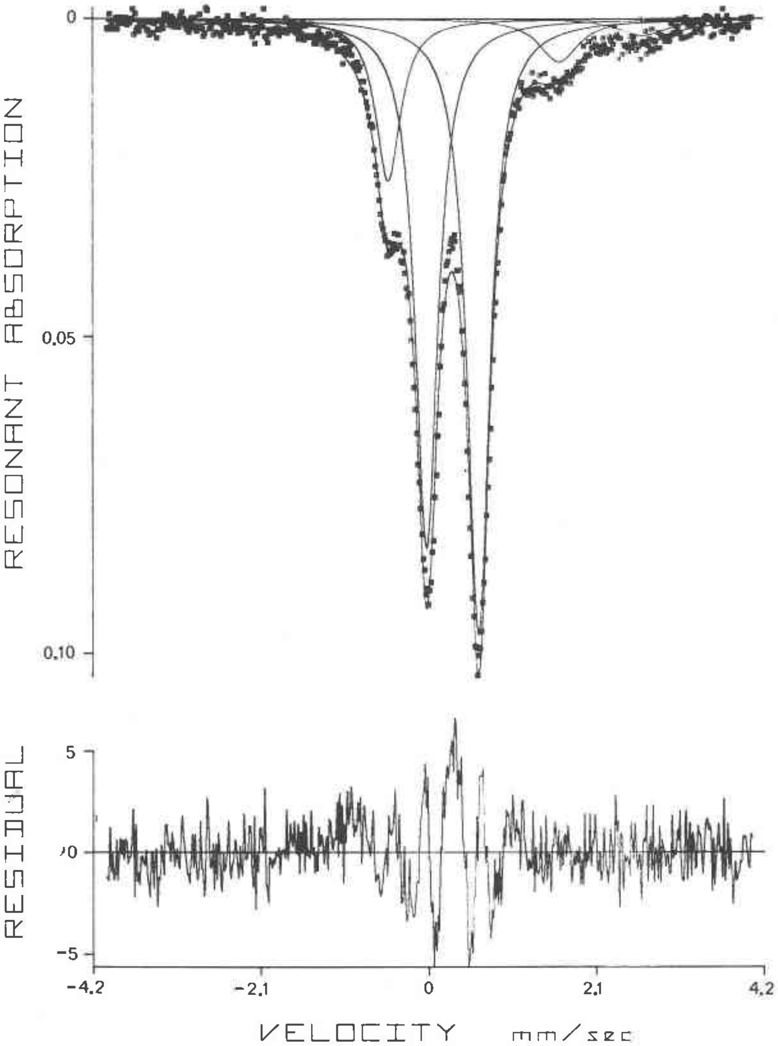

Fig. 4. Mössbauer spectrum of schorlomite from Iivaara alkaline igneous complex, Finland; sample ML. Spectrum is fitted to five peaks.

ciple with the results of Manning and Harris (1970), who, on the basis of optical absorption spectroscopic and electron microprobe data, suggested that Ti^{3+} is abundant in some samples from this locality (San Benito County, California). The results of the present study indicate that considerably smaller amounts of Ti^{3+} are present, approximately one third to one quarter of those estimated by Manning and Harris. Their estimate of the optical absorption extinction coefficient for Ti^{3+} in garnets may be much too small, resulting in large overestimates of the amount of Ti^{3+} in the melanites and schorlomites that they investigated. Alternatively, there may be a large variation in composition of specimens from this locality. Nevertheless, the results of both studies indicate that a substantial amount of Ti^{3+} is present in these samples.

Interpretation of peak B_{IV} in the Mössbauer spectrum

Except for the two samples lowest in Ti (samples O and F), which showed Mössbauer peaks due to dodecahedral ferrous iron only, and the Fe^{2+}-free sample (DW), the remaining samples exhibited a peak in their Mössbauer spectra at about 1.6–1.8 mm/sec, which has been attributed to tetrahedral ferrous iron. The temperature dependence of this peak indicates that it must be associated with Fe^{2+} (ferric peaks are usually invariant with respect to temperature); however, the value for the isomer shift (0.7–0.9 mm/sec at 77 K) appears to be anomalously low, even for tetrahedral Fe^{2+}. Such low values may in part be an artifact of the fitting procedure, because the exact position of the low-velocity peak is not known. On the basis of the change of the low-velocity region of the spectra between 77 K and 298 K (for example, Fig. 6), however, it can be stated that the position of the low-velocity peak could not be in error by as much as 0.3–0.8 mm/sec, which is required to bring the isomer shift into agreement with that of other minerals containing tetrahedral Fe^{2+} (~1.05–1.10 mm/sec at 77 K).

Unusually low values of the isomer shift are often associated with electron-hopping between neighboring Fe cations in a crystal structure. The classic example is magnetite (Kundig and Hargrove, 1969), which has an isomer shift at 298 K of 0.66 mm/sec for octahedral iron cations of average valency, $Fe^{2.5+}$. Iron-rich silicate minerals that may also show this effect include deerite (Frank and Bunbury, 1974) and ilvaite (Grandjean and Gerard, 1975), both of which contain cations with Mössbauer parameters that not only are unusual in value but also have an unusual temperature dependence. Grandjean and Gerard (1975) postulate for ilvaite that the Fe cations, as a result of electron-hopping, change from having a predominantly ferrous-like character at low temperature to having an increasingly ferric-like character as the temperature increases.

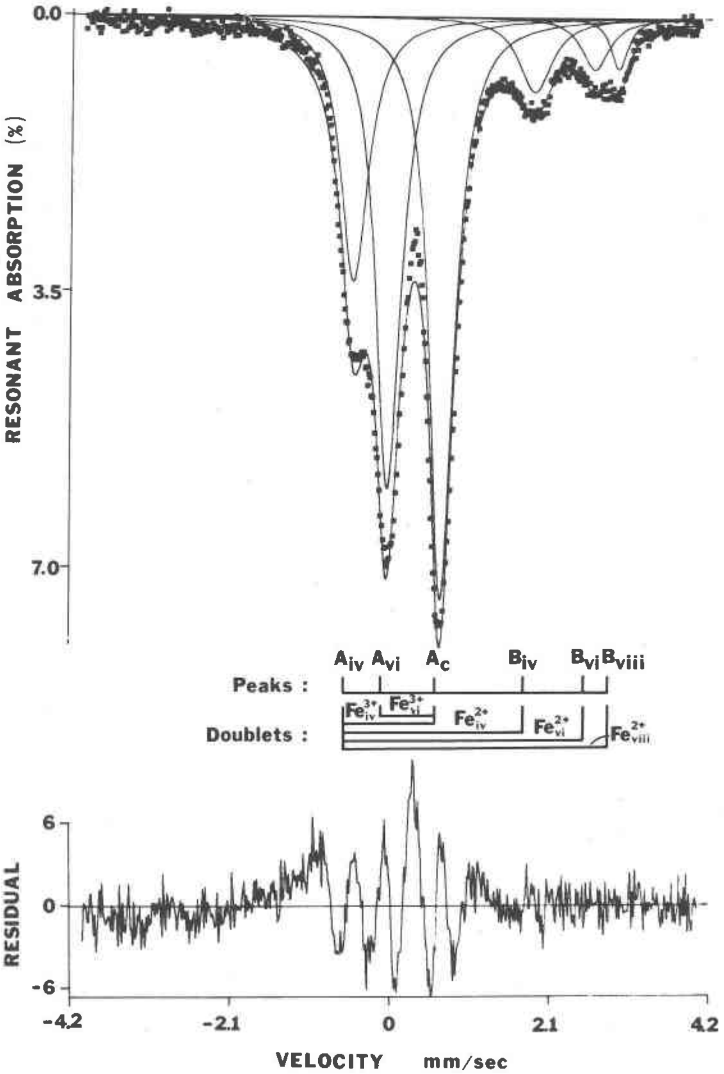

Fig. 5. Mössbauer spectrum of schorlomite from Ardnamurchan, Scotland; sample Ar. Spectrum is fitted to six peaks. Also shown are the labeling scheme for the peaks and the definitions of the doublets for the five distinct types of iron cations.

Table 4. Mössbauer data (peak positions, areas and widths) for garnet samples

		O	F	LB	SB	OL	DW*	K	Iv	ML	R	R*	Ar
$\underline{A}_{IV}$	Position†	-0.630	-0.629	-0.537	abs	-0.539	-0.609	-0.530	-0.521	-0.515	-0.464	-0.579	-0.493
	Area	0.029	0.039	0.061		0.121	0.148	0.148	0.139	0.123	0.188	0.120	0.191
	Width†	0.30	0.30	0.53		0.41	0.36	0.43	0.36	0.37	0.46	0.38	0.43
$\underline{A}_{VI}$	Position	0.016	0.010	-0.048	0.001	-0.046	-0.116	-0.034	-0.042	-0.038	-0.006	-0.103	-0.035
	Area	0.470	0.458	0.446	0.510	0.367	0.362	0.350	0.355	0.369	0.328	0.369	0.309
	Width	0.29	0.29	0.31	0.32	0.33	0.34	0.38	0.34	0.34	0.35	0.38	0.39
$\underline{A}_{c}$	Position	0.602	0.607	0.572	0.605	0.600	0.572	0.648	0.627	0.613	0.668	0.572	0.670
	Area	0.484	0.479	0.478	0.455	0.418	0.490	0.423	0.436	0.428	0.390	0.422	0.370
	Width	0.30	0.30	0.33	0.29	0.34	0.36	0.39	0.34	0.33	0.34	0.37	0.38
$\underline{B}_{IV}$	Position	abs	abs	~1.80	1.656	1.563	abs	1.665	1.617	1.630	1.854	1.330	1.878
	Area			~0.005	0.018	0.045		0.027	0.046	0.052	0.042	0.047	0.066
	Width			~0.50	0.31	0.64		0.44	0.57	0.60	0.37	0.61	0.53
$\underline{B}_{VI}$	Position	abs	abs		2.632	2.619	abs						2.648
	Area				0.017	0.049							0.038
	Width				0.39	0.53							0.45
	Position‡			~2.80				2.720	2.876	2.702	2.710	2.507	
	Area‡			~0.010				0.053	0.024	0.028	0.053	0.042	
	Width‡			~0.50				0.66	0.72	0.79	0.55	0.68	
$\underline{B}_{VIII}$	Position	3.016	3.000		abs	abs	abs						2.973
	Area	0.017	0.024										0.026
	Width	0.34	0.35										0.30
$Fe^{2+}/\Sigma Fe$		0.03	0.05	~0.03	0.07	0.19	0.00	0.16	0.14	0.16	0.19	0.19	0.26
$Fe^{3+}{}_{IV}$§		2.6	3.6	7.8	0.0	7.8	27.6	14.1	15.0	10.2	15.5	17.8	12.2
$Fe^{3+}{}_{VI}$‖		94.0	91.6	89.2	93.0	73.4	72.4	70.0	71.0	73.8	65.6	64.4	61.8
$Fe^{2+}{}_{IV}$¶		0.0	0.0	~1.0	3.6	9.0	0.0	5.4	9.2	10.4	8.4	9.4	13.2
$Fe^{2+}{}_{VI}$¶		0.0	0.0	~2.0**	3.4	9.8	0.0	10.6**	4.8**	5.6**	10.6**	8.4**	7.6
$Fe^{2+}{}_{VIII}$¶		3.4	4.8		0.0	0.0	0.0						5.2

*Data for sample at room temperature.

†Positions and widths in mm/sec.

‡$\underline{B}_{VI}$ and $\underline{B}_{VIII}$ were not differentiated.

§Calculated as area ($\underline{A}_{IV}$ - $\underline{B}_{IV}$ - $\underline{B}_{VI}$ - $\underline{B}_{VIII}$) + area ($\underline{A}_c$ - $\underline{A}_{VI}$).

‖Calculated as 2 × area ($\underline{A}_{VI}$) except for SB, which was calculated as area ($\underline{A}_c$) + area ($\underline{A}_{VI}$ - $\underline{B}_{IV}$ - $\underline{B}_{VI}$).

¶Calculated as 2 × area ($\underline{B}_i$), where $\underline{i}$ = IV, VI or VIII.

**$Fe^{2+}{}_{VI}$ and $Fe^{2+}{}_{VIII}$ were not differentiated.

Hence, it is probable that the low value of the isomer shift and the rapid change in quadrupole splitting with temperature of peak B_{IV} in the garnet spectrum may be related to a change in the character of the cation as a result of electron-hopping between adjacent cations. Most likely this hopping would take place between Fe cations at tetrahedral sites and Fe or Ti cations at adjacent octahedral sites.

Correlation of color and features in the optical absorption spectrum with chemistry

We observed that the color of the garnets varied from orange-brown, which was reasonably transparent in thin section or grain mounts, to a deep purplish red, which was almost opaque. Generally, the variation in color can be correlated with the Ti content, as suggested by Howie and Woolley (1968), but not exactly. Samples DW and Iv, respectively, were orange-brown and deep orange-brown, whereas samples of comparable titanium content (*e.g.*, OL and K) were of the deep red, almost opaque variety. We suggest, however, that a more exact correlation is found between the color and the Fe^{2+}VI content, rather than the Ti content, because the orange-brown colors are found in garnets with only very small amounts of Fe^{2+}VI, whereas the much deeper, redder

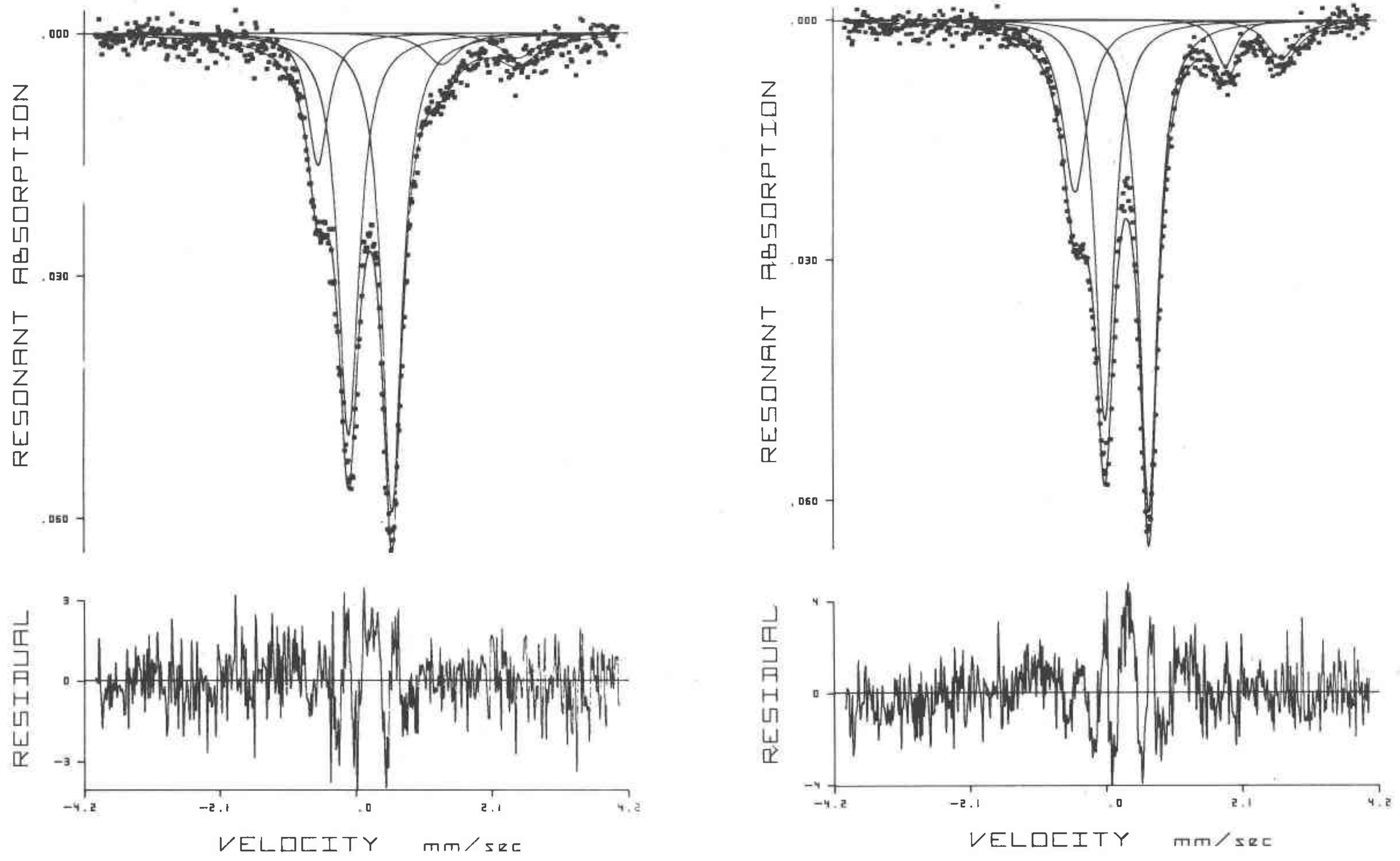

Fig. 6. Mossbauer spectra of schorlomite from Rusinga Island, Uganda; sample R. Spectra are fitted to five peaks. Left spectrum was obtained at 298 K; right spectrum was obtained at 77 K. Note the shift of the ferrous peak, B_{IV}, and the enhancement of peak A_{IV} as a result of cooling the sample to 77 K.

Table 5. Isomer shift and quadrupole splitting data (in mm/sec) for melanites and schorlomites

		O	F	LB	SB	OL	DW*	K	Iv	ML	R	R*	Ar
Fe^{3+}_{IV}	IS	0.16	0.17	0.19	abs	0.21	0.16	0.24	0.23	0.23	0.28	0.17	0.27
	QS	1.23	1.24	1.11		1.14	1.18	1.18	1.15	1.13	1.13	1.15	1.17
Fe^{3+}_{VI}	IS	0.49	0.49	0.44	0.48	0.45	0.41	0.48	0.47	0.46	0.51	0.41	0.50
	QS	0.59	0.59	0.62	0.60	0.65	0.69	0.68	0.67	0.65	0.67	0.68	0.70
Fe^{2+}_{IV}	IS	abs	abs	∼0.80	†	0.69	abs	0.74	0.73	0.73	0.87	0.79‡	0.87
	QS			∼2.35		2.10		2.20	2.14	2.15	2.32	1.43	2.37
Fe^{2+}_{VI}	IS	abs	abs		†	1.22	abs						1.26
	QS					3.16							3.15
	IS§			∼1.30				1.27	1.35	1.27	1.30	1.14	
	QS§			∼3.35				3.26	3.40	3.23	3.17	3.09	
Fe^{2+}_{VIII}	IS	1.37	1.36		abs	abs	abs						1.42
	QS	3.65	3.63										3.47

*Sample at room temperature. Add ∼0.09 mm/sec to IS to make it compatible with samples at 77°K.
†Low-velocity peak not fitted; no calculation possible.
‡Based on the positions of peaks $\underline{A}_{VI}$ and $\underline{B}_{IV}$ rather than $\underline{A}_{IV}$ and $\underline{B}_{IV}$ used for samples at 77°K.
§Fe^{2+}_{VI} and Fe^{2+}_{VIII} were not differentiated.

colors are found in garnets containing substantial Fe^{2+}VI. Further evidence for this point of view is as follows: samples synthesized by Huckenholz (1969), which contain up to 20 weight percent Ti but negligible Fe^{2+}, all exhibit light yellow to orange colors in grain mounts. Furthermore, a sample of SB, which was heated in a ZrO_2 electrochemical cell to measure its intrinsic oxygen fugacity (Virgo *et al.*, in preparation), underwent a color change from almost opaque to pale yellow without apparently decomposing. Whereas X-ray and electron microprobe analyses indicated that the overall composition of this garnet did not change, the Mössbauer spectrum (Fig. 8) and the optical spectrum (Fig. 9) before and after treatment in the cell were obviously different. The loss of the Fe^{2+} peaks in the Mössbauer spectrum correlates

Table 6. $Fe^{2+}/\Sigma Fe$ ratios for melanites and schorlomites

Sample	$Fe^{2+}/\Sigma Fe$			$Ti^{3+}/\Sigma Ti$		Reference for Wet Chemical Analysis
	Möss	EMP	Wet*	EMP-Möss	Wet-Möss	
O	0.03	0.01	...	0.00	...	...
F	0.05	0.06	(0.06)	0.10	(0.10)	G. Cammann (unpublished)
LB	∼0.03	0.02	0.07	0.00	0.20	Howie and Woolley (1968)
SB	0.07	0.17	(0.12)	0.24	(0.12)	Howie and Woolley (1968)
OL	0.18	0.17	...	0.00	...	...
DW	0.00	0.00	(0.04)	0.00	(0.07)	Howie and Woolley (1968)
K	0.16	0.17	0.16	0.02	0.00	G. Cammann (unpublished)
Iv	0.14	0.18	...	0.07	...	...
ML	0.16	0.19	0.18	0.05	0.04	Lehijärvi (1960)
R	0.19	0.21	(0.20)	0.03	(0.02)	Howie and Woolley (1968)
Ar	0.26	0.26	0.27	0.00	0.01	Howie and Woolley (1968)
GN3†	0.00	...	0.04	...	var‡	Whipple (1973)
GN4†	0.01	...	0.09	...	var‡	Whipple (1973)
GN6†	0.03	...	0.05	...	0.17	Whipple (1973)
No. 8, E.D.§	0.13	...	0.15	...	0.03	Dowty (1971)

*Values in parentheses are for sample from same locality, rather than for same sample.
†Samples investigated by E. R. Whipple (see Whipple, 1973). GN3 from Magnet Cove, Arkansas; GN4 from Morocco (see also Burns, 1972); GN6 from Oka, Quebec, Canada.
‡Variable owing to zoning.
§Sample investigated by E. Dowty (see Dowty, 1971). No. 8 from Iron Hill, Colorado.

with the change from a very deep red to yellow, which is also indicated by a shift of the absorption edge in the optical spectrum to much higher energy. The band at 5000 cm^{-1} also disappears from the spectrum, suggesting that this band is also related to ferrous iron. Based on its position, this band is interpreted as due to the $e \rightarrow t_2$ transition in tetrahedral Fe^{2+}.

It appears that the presence of octahedral and tetrahedral Fe^{2+} in the garnet is largely responsible for the important features in the optical absorption spectrum, as well as the color of the garnet. The shift of the absorption edge to lower energy, and similar color changes with increasing Fe^{2+}, are also observed in Si^{4+}-doped yttrium iron garnets, where Fe^{2+} is present to preserve charge-balance requirements in the garnet structure (Wickersheim and Lefever, 1962). In both cases, the presence of Fe^{2+} must enhance the cation–anion charge-transfer process responsible for the absorption edge.

Summary of the crystal chemistry of melanites and schorlomites

The Mössbauer spectra of the garnets are invaluable for locating the different Fe cations in the garnet structure. By making use of known crystal-chemical principles in conjunction with these data, details of the location of all elements in these garnets can be inferred, except for the distribution of Al and Ti^{4+} between octahedral and tetrahedral sites and in certain cases the distribution of Fe^{2+} and Mg between the dodecahedral and octahedral sites.

The assumptions that are inherent in the summary of the location of cations in the garnets (Table 7) include:

(1) The order of assigning of divalent cations between dodecahedral and octahedral sites is according to ionic radii; *i.e.*, Mg^{2+} was assigned to the octahedral sites first, and Ca^{2+} last. This assumption ignores the possibility of an order–disorder phenomenon, especially for Fe^{2+} and Mg^{2+}, between the two sites.

(2) Any Ti^{3+} is located exclusively in the octahedral site. On the basis of ionic size and octahedral preference energy, as a result of the crystal-field stabilization energy for Ti^{3+}, it appears unlikely that Ti^{3+} would substantially populate the tetrahedral site, in view of the lack of preference that Ti^{4+} shows for the tetrahedral site (Huggins *et al.*, 1977).

(3) The site populations of Fe cations are assumed to be directly proportional to the area ratios shown in Table 4. This requires that there be no significant difference between Fe^{2+} and Fe^{3+} recoil-free fractions at 77 K.

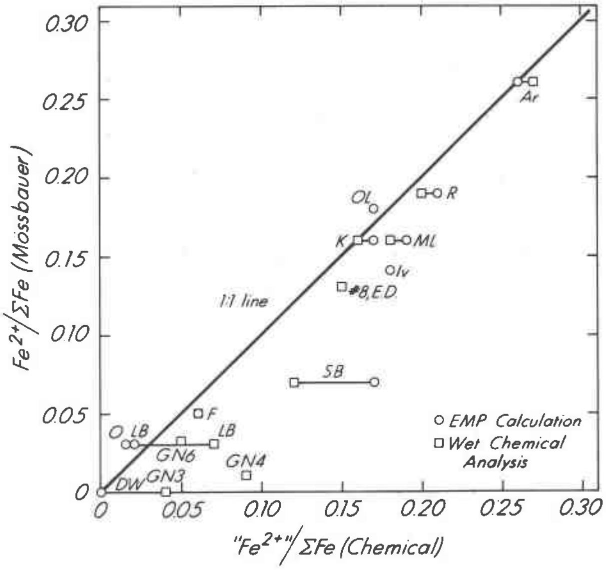

Fig. 7. Comparison of $Fe^{2+}/\Sigma Fe$ ratios as determined by Mössbauer spectroscopy and by chemical methods for melanite and schorlomite garnets. Significant deviation to the right of the 1:1 line probably indicates the presence of Ti^{3+}.

In all samples, it is necessary to have some Mg^{2+} or Fe^{2+} or both in the octahedral sites, but in only three samples (O, SB, and DW) is Mn required to be on the octahedral site, and in only two samples (SB and DW) is Ca required to be on that site. This anomalous property of DW and SB has already been noted, and any explanation other than the coupled substitutions

$$Ca^{2+}VI + Ti^{4+}VI \rightleftarrows 2M^{3+}VI$$

$$Mn^{2+}VI + Ti^{4+}VI \rightleftarrows 2M^{3+}VI$$

does not appear plausible. Previous evidence for Mn^{2+} at the octahedral sites in garnets has been presented by Geller (1967), but evidence for octahedral Ca^{2+}, except possibly in garnets formed at very high pressures (Ringwood and Seabrook, 1963), is lacking. Sample O indicates that Fe^{2+} is found in the dodecahedral site at the expense of Mn, in contrast to all other samples investigated in this study. This difference may be best explained if the octahedral Mn is in fact in the trivalent state. Consequently, the $Fe^{2+}/\Sigma Fe$ calculated from the electron microprobe analysis would be increased from 0.015 to 0.034, and this result would be in exact agreement with the value for $Fe^{2+}/\Sigma Fe$ as measured by Mössbauer spectroscopy.

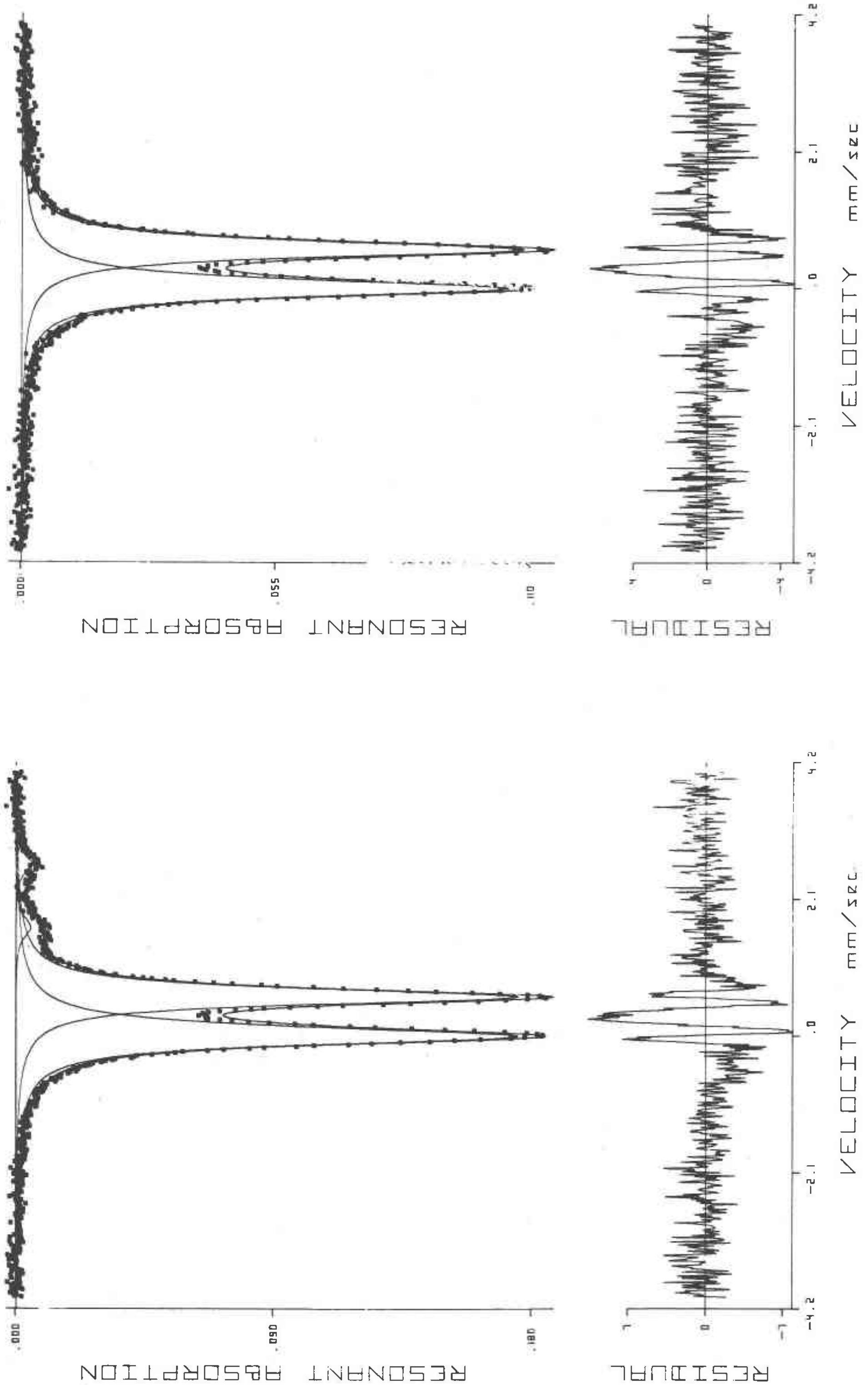

Fig. 8. Mössbauer spectra of sample SB before (left) and after (right) treatment in the ZrO_2 electrochemical cell (Virgo *et al.*, in preparation).

At the tetrahedral site, only Fe^{2+} of the divalent cations is considered as substituting. Dowty (1971) proposed the substitution

$$2M^{3+}\mathrm{VI} + Si^{4+}\mathrm{IV} \rightleftarrows 2Ti^{4+}\mathrm{VI} + Fe^{2+}\mathrm{IV}$$

to account for tetrahedral Fe^{2+}. However, in view of the incompatibility of the size of Fe^{2+} cations and tetrahedral sites usually occupied by Si^{4+}, it is likely that the Fe cation actually entered the tetrahedral site not as Fe^{2+}, but as Fe^{3+}. Hence, it is suggested that the extra electron now on this tetrahedral Fe cation results from its being trapped in one of two possible electron-hopping centers,

$$Fe^{2+}\mathrm{VI} + Fe^{3+}\mathrm{IV} \rightleftarrows Fe^{3+}\mathrm{VI} + Fe^{2+}\mathrm{IV}$$

$$Ti^{3+}\mathrm{VI} + Fe^{3+}\mathrm{IV} \rightleftarrows Ti^{4+}\mathrm{VI} + Fe^{2+}\mathrm{IV}$$

and that the original coupled substitutions actually resulted in Fe^{2+}VI or Ti^{3+}VI by means of the following mechanisms:

$$Fe^{2+}\mathrm{VI} + Ti^{4+}\mathrm{VI} \rightleftarrows 2M^{3+}\mathrm{VI}$$

$$Ti^{3+}\mathrm{VI} \rightleftarrows M^{3+}\mathrm{VI}.$$

In this respect, the unusual Mössbauer parameters for the Fe^{2+}IV absorption, suggestive of electron-hopping, have already been discussed. Obviously, because similar electron-hopping and substitution mechanisms are not possible, other tetrahedrally-coordinated divalent cations need not be considered.

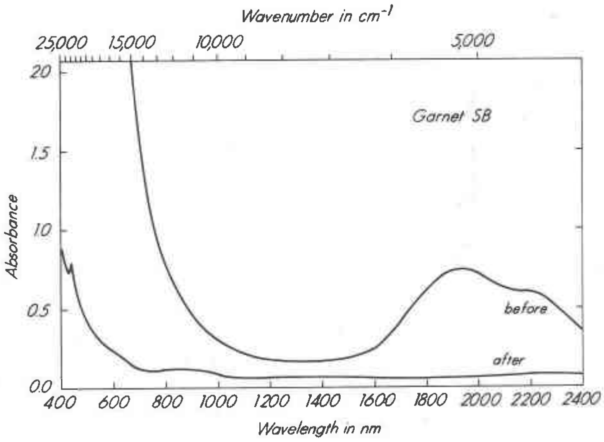

Fig. 9. Optical absorption spectra of sample SB before and after treatment in the ZrO_2 electrochemical cell (Virgo *et al.*, in preparation).

Distribution of Fe cations between octahedral and tetrahedral sites

In order to compare the distribution of Fe cations between the octahedral and tetrahedral sites for the natural garnets with that for the synthetic Ti garnets (Huggins *et al.*, 1977), additional crystal-chemical complexities of the natural garnets must be considered. For this reason, a number of different Fe distribution models have been considered for the natural garnets to allow for the presence of Fe^{2+} and in-

Table 7. Location of cations at crystallographic positions in natural melanite and schorlomite garnets*

	O	F	SB	OL	DW	K	Iv	ML	R	Ar
					Tetrahedral Cations					
Si	2.900	2.924	2.834	2.623	2.276	2.470	2.472	2.492	2.442	2.250
Fe^{3+}	0.038	0.046	0.000	0.121	0.356	0.203	0.224	0.151	0.223	0.167
Fe^{2+}	0.000	0.000	0.047	0.140	0.000	0.078	0.138	0.154	0.121	0.181
Al + Ti^{4+}	0.062	0.030	0.119	0.116	0.368	0.250	0.166	0.203	0.214	0.402
					Octahedral Cations					
Ti^{3+}	0.000	0.015	0.131	0.000	0.000	0.022	0.060	0.044	0.029	0.000
Fe^{3+}	1.366	1.171	1.220	1.142	0.934	1.006	1.062	1.092	0.943	0.845
Al + Ti^{4+}	0.550	0.749	0.450	0.647	0.929	0.775	0.738	0.710	0.798	1.016
Fe^{2+}	0.000	0.000	0.045	0.152	0.000	0.197	0.140	0.154	0.230	0.104
Mg	0.054	0.065	0.090	0.059	0.107					0.035
Mn	0.030†	0.000	0.009	0.000	0.006	0.000	0.000	0.000	0.000	0.000
Ca	0.000	0.000	0.055	0.000	0.024	0.000	0.000	0.000	0.000	0.000
					Dodecahedral Cations					
Mg	0.000	0.005	0.000	0.000	0.000	0.072	0.052	0.052	0.037	0.030
Fe^{2+}	0.049	0.061	0.000	0.001	0.000					0.071
Mn	0.039	0.020	0.000	0.029	0.000	0.030	0.016	0.018	0.024	0.025
Ca	2.912	2.914	3.000	2.970	3.000	2.898	2.932	2.930	2.939	2.874

*Garnet specimen LB not included as small amounts of Fe^{2+} cannot be measured accurately.
†Octahedral Mn is possibly in trivalent state in this garnet.

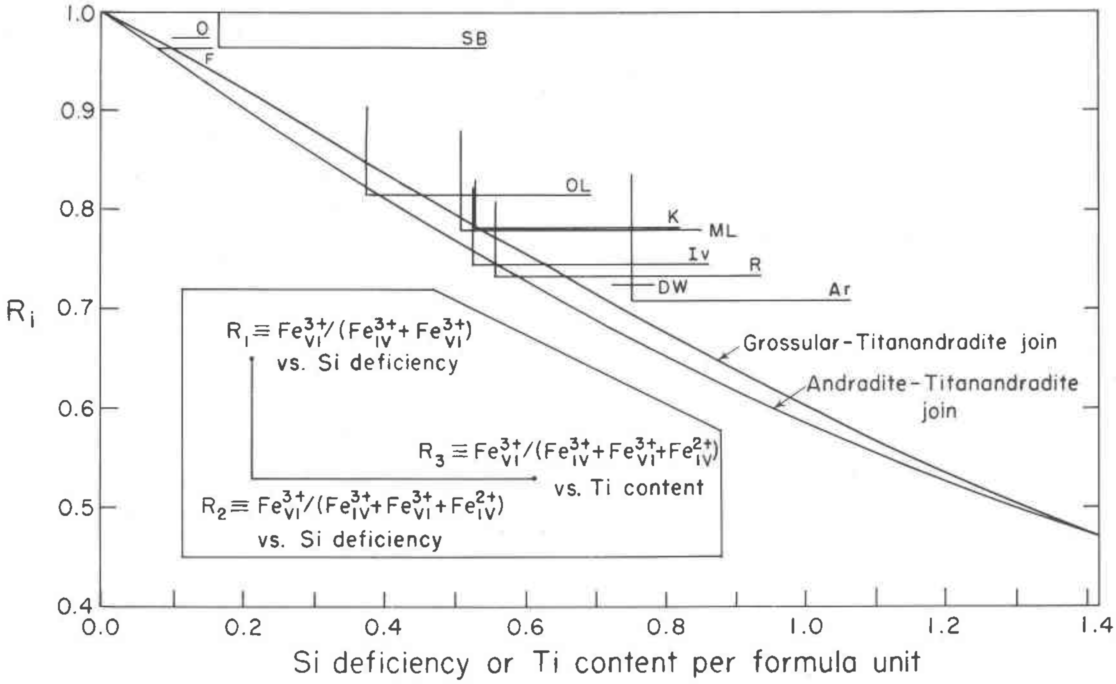

Fig. 10. Comparison of three different ferric distribution parameters for the natural samples with the distribution trends established for synthetic garnets synthesized above 1200°C (Huggins *et al.*, 1977).

equality of the Si deficiency and Ti content. Three such models are shown in Figure 10.

Figure 10 is a composite plot of $Fe^{3+}VI/(Fe^{2+}IV + \Sigma Fe^{3+})$ against titanium content. The data for the natural samples are compared with curves representing $Fe^{3+}VI/\Sigma Fe^{3+}$ values for the synthetic GR–TIAN and AN–TIAN joins based on the distributions quenched at temperatures above 1200°C (Huggins *et al.*, 1977). In view of the order of tetrahedral-site preference, Al > Fe > Ti, these curves are not expected to change greatly with decreasing temperature, because Fe has the intermediate site preference; *i.e.* most of the change in distribution with temperature can be expected to involve Al and Ti, rather than Fe. Figure 10 shows that the ratio $Fe^{3+}VI/(Fe^{2+}IV + \Sigma Fe^{3+})$ plotted against Si deficiency agrees best with the curves for the synthetic samples. It is not unexpected that Si deficiency rather than Ti content is the proper parameter for the abscissa because, of course, Si deficiency rather than Ti content is the correct measure of the number of tetrahedral sites available for exchange. However, the fact that the best-fitting ordinate parameter is $Fe^{3+}VI/(Fe^{2+}IV + \Sigma Fe^{3+})$ and not $Fe^{3+}VI/\Sigma Fe^{3+}$ implies that $Fe^{2+}IV$ cannot be differentiated from $Fe^{3+}IV$ for the purposes of the cation-exchange processes, and that all tetrahedral and octahedral cations, except Si^{4+} and probably $Mg^{2+}VI$, take part in the cation-exchange phenomena between the octahedral and tetrahedral sites. For this latter reason, at high temperatures the Fe and Ti cations are probably essentially Fe^{3+} or Ti^{4+}. This observation implies that the extra electrons associated with Fe^{2+} or Ti^{3+} at room temperature are not localized but are able to move rapidly from one cation to another at high temperatures.

Of the ten samples plotted in Figure 10, only SB appears to be significantly removed from the curves for the synthetic garnets. Because this sample may have a much lower temperature paragenesis than the other samples, its cation distribution probably did not reach equilibrium. As discussed previously (Huggins *et al.*, 1977), the anomalous value for $Fe^{3+}VI/(Fe^{2+}IV + \Sigma Fe^{3+})$ for this sample may be a reflection of the distribution initially generated by the low-temperature reaction responsible for the formation of the garnet. Subsequently, owing to the low temperature of origin, this initial distribution was never equilibrated.

The other samples, however, appear to be consistent with a higher-temperature origin at which an equilibrium cation distribution could be attained. Indeed, as might be predicted from the order of tetrahedral-site preference, Al > Fe > Ti, those garnets with greater total Al contents (*e.g.*, K, DW, Ar) do have values of Fe^{3+}VI/(Fe^{2+}IV + ΣFe^{3+}) significantly higher with respect to the curves for the synthetic samples (Fig. 10) than the Al-poor samples (*e.g.*, OL, ML, Iv, and R). This observation reinforces the conclusion that the order of tetrahedral-site preference for both natural and synthetic titanium silicate garnets is Al > Fe > Ti.

Conclusions

The presence of up to five distinct Fe absorptions in the Mössbauer spectrum and the deviation of the chemistry of natural melanites and schorlomites from the regular silicate garnet crystal chemistry indicate that no single coupled substitution is responsible for the introduction of all the Ti into the garnet structure. Rather, it appears that a combination of the following coupled substitutions may be used for introducing Ti into the structure:

(1) $Ti^{4+} \rightleftarrows Si^{4+}$ (concomitant with Al, Fe, and Ti exchange reactions between the octahedral and tetrahedral sites).

(2) M^{2+}VI + Ti^{4+} VI $\rightleftarrows 2M^{3+}$ (M^{2+} = Mg, Fe^{2+}, Mn?, Ca?).

(3) Ti^{3+}VI $\rightleftarrows M^{3+}$ VI.

(4) Substitutions like 2 and 3 responsible for the formation of Fe^{2+}IV.

(5) NaVIII + Ti^{4+}VI $\rightleftarrows M^{2+}$VIII + M^{3+}VI (to account for the possible presence of any Na).

The relative proportions of the different substitution mechanisms (1–4) for the garnets investigated are shown in Figure 11. The substitution of type 1 dominates; next in importance is usually type 2, although as the Ti and Fe^{2+} contents increase type 4 becomes increasingly important. Owing to electron-hopping at high temperatures, the relative amounts of substitutions 2 and 3 found at low temperature probably bear no relation to the amounts of these substitutions occurring at the time of the garnet's formation.

This study has also shown (Fig. 7) that most of the reduced cations found in chemical analyses of the garnets are Fe^{2+} cations. However, the presence of minor amounts of Ti^{3+} in some samples, and significant amounts in sample SB, appears necessary to account for the additional amounts of reduced cations found in chemical analyses compared with the number of Fe^{2+} cations found in the Mössbauer spectra.

The presence of Fe^{2+} and possibly Ti^{3+} on octahedral sites suggests that the garnets formed under conditions of oxygen fugacity lower than that which ensures only Fe^{3+} or Ti^{4+} at the octahedral site. Evidence reinforcing this inference is presented by Huckenholz *et al.* (in preparation) and Virgo *et al.* (in preparation), who found that natural melanites and schorlomites do indeed form under conditions of low oxygen fugacity. From these studies, we conclude that the small amounts of Fe^{2+} in unusual sites for

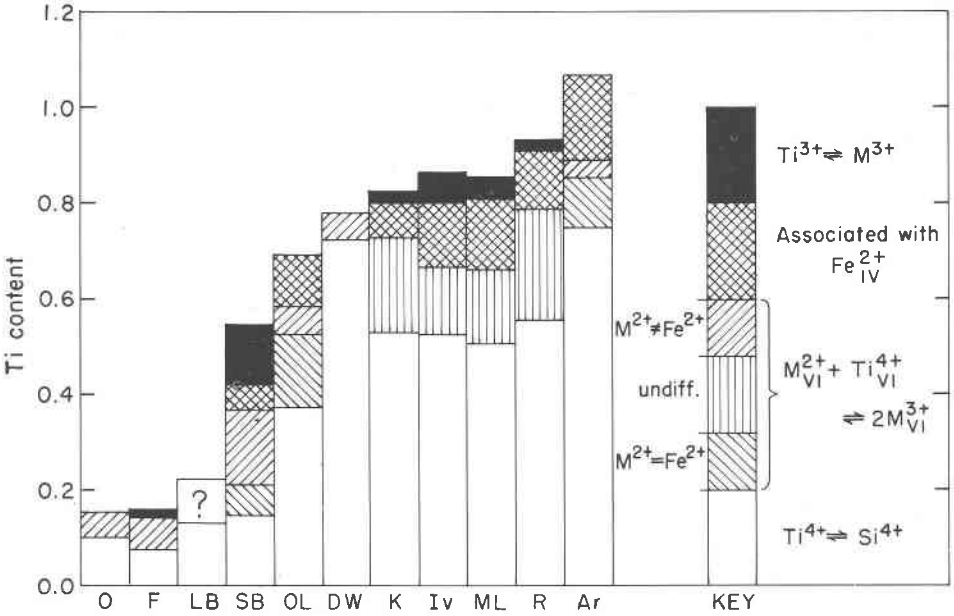

Fig. 11. Histogram indicating the relative proportions of the different coupled-substitution reactions for the melanite and schorlomite garnets as found at low temperature.

Table Al. Supplementary electron microprobe analyses: zoned garnets and No. 4562

	4718*		KO*		AD*			
	a	b	a	b	a	b	c	d
SiO_2	33.50	32.35	33.39	32.38	32.58	32.23	30.75	28.66
TiO_2	6.35	8.71	6.75	9.41	6.97	9.06	10.57	14.21
Al_2O_3	2.22	2.03	2.27	2.13	2.47	2.86	2.27	2.20
Fe_2O_3†	25.06	24.02	24.26	23.17	24.10	22.17	22.97	21.54
MgO	0.35	0.39	0.37	0.41	0.63	0.83	0.77	1.04
MnO	0.41	0.43	0.39	0.43	0.34	0.36	0.37	0.28
CaO	33.24	33.34	33.60	33.39	33.22	33.92	33.04	32.54
Totals	101.21	100.99	101.02	101.30	100.30	101.43	100.75	100.39

	MC*		4562	SB*			
	a	b		a	b	c	d
SiO_2	34.42	28.16	27.85	34.85	33.01	34.10	33.76
TiO_2	2.87	14.81	13.75	8.25	9.60	6.54	5.70
Al_2O_3	2.47	1.20	2.32	6.41	1.28	0.67	0.35
Fe_2O_3†	25.01	22.27	20.54	14.60	19.94	23.79	24.64
MgO	0.53	1.05	1.09	1.13	0.73	0.52	0.53
MnO	0.28	0.66	0.30	0.14	0.14	0.10	0.09
CaO	34.07	32.76	32.67	34.96	33.77	33.07	32.75
Totals	99.65	100.91	98.52	100.34	98.48	98.79	97.81

*Zoned sample. Analyses shown are averages for distinct zones.
†All iron as Fe_2O_3.

Fe^{2+} in the garnet structure, rather than the larger amounts of Fe^{3+}, are diagnostic of the oxygen fugacity at the time of formation. As discussed elsewhere (Virgo *et al.*, in preparation), this result has important petrological implications for the origin of rocks containing melanites and schorlomites, which have hitherto been thought to originate under oxidizing conditions.

The distribution of cations between the octahedral and tetrahedral sites may also have important implications for obtaining information concerning the thermal history of rocks containing titanium–silicate garnets. Unfortunately, the effect of temperature is likely to be more pronounced with the Al and Ti distribution rather than Fe, because of the order of tetrahedral-site preference, Al > Fe > Ti, in which Fe is intermediate. This order of site preference, established for the simpler synthetic garnet systems, is compatible with most of the natural samples, indicating that such melanites and schorlomites have an equilibrated cation distribution.

Finally, the crystal chemistry of melanites and schorlomites results from two processes that occur simultaneously at high temperatures. These processes are cation-exchange reactions, which involve the distribution of Al, Fe, and Ti cations between octahedral and tetrahedral sites, and electron-hopping between Fe and Ti cations. The crystal-chemical details observed at room temperature reflect these two processes. However, the observation of certain of these details, such as Fe^{2+}IV and the inferred coexistence of Ti^{3+} and Fe^{3+}, possibly results from the arrested state of the processes at room temperature. Hence, the observed complexity of the crystal chemistry of melanites and schorlomites can be understood in terms of both processes if allowance is made for the temperature of observation.

Appendix

Electron microprobe analyses for garnets that are zoned or were not used for Mössbauer experiments are given in Table Al.

Acknowledgements

We thank R. A. Howie, Th. G. Sahama, J. S. White, Jr., S. O. Agrell and M. Rosenhauer for garnet samples. The manuscript benefitted from discussions and reviews by Y. Ohashi and H. S. Yoder, Jr.

References

Amthauer, G., H. Annersten and S. S. Hafner (1976) The Mössbauer spectra of ^{57}Fe in silicate garnets. *Z. Kristallogr.*, *143*, 14–55.

Burns, R. G. (1972) Mixed valencies and site occupancies of iron in silicate minerals from Mössbauer spectroscopy. *Can. J. Spectrosc.*, *17*, 51–59.

——— and V. M. Burns (1971) Study of the crystal chemistry of titaniferous garnets by Mössbauer spectroscopy. *Geol. Soc. Am. Abstr. Programs, 3,* 519–520.

———, F. E. Huggins and H. G. Drickamer (1972) Applications of high-pressure Mössbauer spectroscopy to mantle mineralogy. *24th. Int. Geol. Congr., Montreal, Sect. 14,* 113–123.

Dowty, E. (1971) Crystal chemistry of titanian and zirconian garnet: I. Review and spectral studies. *Am. Mineral., 56,* 1983–2009.

Erickson, R. L. and L. V. Blade (1963) Geochemistry and petrology of the alkalic igneous complex at Magnet Cove, Arkansas. *U. S. Geol. Surv. Prof. Pap., 425.*

Finger, L. W. (1972) The uncertainty in the calculated ferric iron content of a microprobe analysis. *Carnegie Inst. Wash. Year Book, 71,* 600–603.

——— and C. G. Hadidiacos (1972) Electron microprobe automation. *Carnegie Inst. Wash. Year Book, 71,* 598–600.

Frank, E. and D. St. P. Bunbury (1974) A study of deerite by the Mössbauer effect. *J. Inorg. Nucl. Chem., 36,* 1725–1730.

Geller, S. (1967) Crystal chemistry of the garnets. *Z. Kristallogr., 125,* 1–47.

Grandjean, F. and A. Gerard (1975) Analysis by Mössbauer spectroscopy of the electronic hopping process in ilvaite. *Solid State Commun., 16,* 553-556.

Howie, R. A. and A. R. Woolley (1968) The role of titanium and the effect of TiO_2 on the cell size, refractive index and specific gravity in the andradite–melanite–schorlomite series. *Mineral. Mag., 36,* 775–790.

Huckenholz, H. G. (1969) Synthesis and stability of Ti-andradite. *Am J. Sci., 267A,* 209–232.

Huggins, F. E., D. Virgo and H. G. Huckenholz (1977) Titanium-containing silicate garnets. I. The distribution of Al, Fe^{3+} and Ti^{4+} between octahedral and tetrahedral sites. *Am. Mineral., 62,* 475–490.

Kundig, W. and R. S. Hargrove (1969) Electron hopping in magnetite. *Solid State Commun., 7,* 223–227.

Lehijärvi, M. (1960) The alkaline district of Iivaara, Kuusamo, Finland. *Bull. Comm. Geol. Finlande, 185.*

Manning, P. G. and D. C. Harris (1970) Optical-absorption and electron-microprobe studies of some high-Ti andradites. *Can. Mineral., 10,* 260–271.

Moore, R. K. and W. B. White (1971) Intervalence electron transfer effects in the spectra of the melanite garnets. *Am. Mineral., 56,* 826–840.

Novak, G. A. and G. V. Gibbs (1971) The crystal chemistry of the silicate garnets. *Am. Mineral., 56,* 791–825.

Ringwood, A. E. and M. Seabrook (1963) High-pressure phase transformations in germanate pyroxenes and related compounds. *J. Geophys. Res., 68,* 4601–4609.

Whipple, E. R. (1973) *Quantitative Mössbauer Spectra and Chemistry of Iron.* Ph.D. Thesis, Massachusetts Institute of Technology, Cambridge, Massachusetts.

Wickersheim, K. A. and R. A. Lefever (1962) Absorption spectra of ferric iron-containing oxides. *J. Chem. Phys., 36,* 844–850.

Zedlitz, O. (1933) Über titanreichen Kalkeisengranat. *Zentralbl. Mineral. Abt. A,* 225–239.

Manuscript received, October 7, 1976; accepted for publication, February 25, 1977.